Inorg. Chem. **2002**, *41*, 3553–3559

Reactive Intermediates Relevant to the Carbonylation of $CH_3Mn(CO)_5$. Activation Parameters for Key Dynamic Processes

Steve M. Massick, Verena Mertens, Jon Marhenke, and Peter C. Ford*

Department of Chemistry and Biochemistry University of California, Santa Barbara, Santa Barbara, California 93106

Received February 11, 2002

Reported is a time-resolved infrared and optical kinetics investigation of the transient species $CH_3C(O)Mn(CO)_4$ ($\mathbf{I_{Mn}}$) generated by flash photolysis of the acetyl manganese pentacarbonyl complex $CH_3C(O)Mn(CO)_5$ ($\mathbf{A_{Mn}}$) in cyclohexane and in tetrahydrofuran. Activation parameters were determined for CO trapping of $\mathbf{I_{Mn}}$ to regenerate $\mathbf{A_{Mn}}$ (rate $= k_{CO}$ [CO][$\mathbf{I_{Mn}}$]) as well as the methyl migration pathway to form methylmanganese pentacarbonyl CH_3-$Mn(CO)_5$ ($\mathbf{M_{Mn}}$) (rate $= k_M$[$\mathbf{I_{Mn}}$]). These values were $\Delta H^{\ddagger}_{CO} = 31 \pm 1$ kJ mol^{-1}, $\Delta S^{\ddagger}_{CO} = -64 \pm 3$ J mol^{-1} K^{-1}, $\Delta H^{\ddagger}_{M} = 35 \pm 1$ kJ mol^{-1}, and $\Delta S^{\ddagger}_{M} = -111 \pm 3$ J mol^{-1} K^{-1}. Substantially different activation parameters were found for the methyl migration kinetics of $\mathbf{I_{Mn}}$ in THF solutions where $\Delta H^{\ddagger}_{M} = 68 \pm 4$ kJ mol^{-1} and $\Delta S^{\ddagger}_{M} = 10 \pm 10$ J mol^{-1} K^{-1}, consistent with the earlier conclusion (Boese, W. T.; Ford, P. C. *J. Am. Chem. Soc.* **1995**, *117*, 8381–8391) that the composition of $\mathbf{I_{Mn}}$ is different in these two media. The possible isotope effect on k_M was also evaluated by studying the intermediates generated from flash photolysis of $CD_3C(O)Mn(CO)_5$ in cyclohexane, but this was found to be nearly negligible (k_M^h/k_M^d (298 K) $= 0.97 \pm 0.05$, $\Delta H^{\ddagger}_{M}{}^{d} = 37 \pm 4$ kJ mol^{-1}, and $\Delta S^{\ddagger}_{M}{}^{d} = -104 \pm 12$ J mol^{-1} K^{-1}). The relevance to the migratory insertion mechanism of $CH_3Mn(CO)_5$, a model for catalytic carbonylations, is discussed.

Introduction

The reaction of carbon monoxide with a metal−alkyl M−R to form metal−acyl complex M−C(O)R is the key carbon−carbon bond formation step in industrially important catalytic carbonylations such as alkene hydroformylation and acetic acid synthesis from methanol.[1,2] An early model of such "migratory insertion" was the reaction of methylmanganese pentacarbonyl $CH_3Mn(CO)_5$ ($\mathbf{M_{Mn}}$) with various ligands to generate the acyl complexes (eq 1),[3−5] and the mechanism of this and related reactions has subsequently been the subject of a number of experimental[6−12] and computational[13] studies. An overview of these studies indicates several unresolved issues. A key one is that, while the reaction has been shown to proceed by methyl migration to an adjacent coordinated carbonyl (rather than CO insertion into the Mn−alkyl bond), the nature of the intermediate(s) of this step remains uncertain. The reason is straightforward; such intermediates are generally only present in low steady-

(1) Parshall, G. W.; Ittel, S. D. *Homogeneous Catalysis*; John Wiley and Sons: New York, 1992.
(2) *Applied Homogeneous Catalysis with Organometallic Compounds: A Comprehensive Handbook in Two Volumes*; Cornils, B.; Herrmann, W. A., Eds.; VCH: Weinheim, Germany, 1996.
(3) Calderazzo, F. *Angew. Chem., Int. Ed. Engl.* **1977**, *16*, 299−311 and references therein.
(4) (a) Mawby, R. J.; Basolo, F.; Pearson, R. G. *J. Am. Chem. Soc.* **1964**, *86*, 3994−9. (b) Mawby, R. J.; Basolo, F.; Pearson, R. G. *J. Am. Chem. Soc.* **1964**, *86*, 5043−4.
(5) (a) Kraihanzel, C. S.; Maples, P. K. *J. Am. Chem. Soc.* **1965**, *87*, 5267−5268; *Inorg. Chem.* **1968**, *7*, 1806−15.
(6) Butts, S. B.; Strauss, S. H.; Holt, E. M.; Stimson, R. E.; Alcock, N. W.; Shriver, D. F. *J. Am. Chem. Soc.* **1980**, *102*, 5093−5100.
(7) Flood, T. C.; Jensen, J. E.; Statler, J. A. *J. Am. Chem. Soc.* **1981**, *103*, 4410−14.
(8) Booth, B. L.; Lewis, E. J. R. *J. Chem. Soc., Dalton Trans.* **1982**, 417−421.
(9) Nolan, S. P.; Lopez de la Vega, R.; Hoff, C. D. *J. Am. Chem. Soc.* **1986**, *108*, 7852−3.
(10) (a) Cotton, J. D.; Markwell, R. D. *Organometallics* **1985**, *4*, 937−9. (b) Cotton, J. D.; Markwell, R. D. *J. Organomet. Chem.* **1990**, *388*, 123−132. (c) Bent, T. L.; Cotton, J. D. *Organometallics* **1991**, *10*, 3156−66.
(11) Andersen, J.-A. M.; Moss, J. R. *Organometallics* **1994**, *13*, 5013−20. (b) Moss, J. R. *J. Mol. Catal. A: Chem.* **1996**, *107*, 169−174.
(12) (a) Cavell, K. J. *Coord. Chem. Rev.* **1996**, *155*, 209−243. (b) Collman, J. P.; Hegedus, L. S.; Norton, J. R.; Finke, R. G. *Principles and Applications of Organotransition Metal Chemistry;* University Science Books: Mill Valley, CA, 1987; Chapter 6.
(13) (a) Ziegler, T.; Versluis, L.; Tschinke, V. *J. Am. Chem. Soc.* **1986**, *108*, 612−7. (b) Axe, F. U.; Marynick, D. S. *Organometallics* **1987**, *6*, 572−580. (c) Ujaque, G.; Maseras, F.; Lledos, A.; Contreras, L.; Pizzano, A.; Rodewald, D.; Sanchez, L.; Carmona, E.; Monge, A.; Ruiz, C. *Organometallics* **1999**, *18*, 3294−3305. (d) Derecskei-Kovacs, A.; Marynick, D. S. *J. Am. Chem. Soc.* **2000**, *122*, 2078−86.

10.1021/ic020116r CCC: $22.00
Published on Web 06/01/2002

state concentrations during the reaction and are rarely directly observable via spectroscopic techniques. A second issue has to do with solvent effects. Migratory insertion rates in this system (and many related complexes)[14] are markedly accelerated in more polar solvents,[4,10,14] yet the exact role played by solvent in the intimate mechanism has long been a point of disagreement. These types of questions have led us to use time-resolved spectroscopy to interrogate the nature and reaction dynamics of reactive intermediates in migratory insertions such as that represented by eq 1.[15−18]

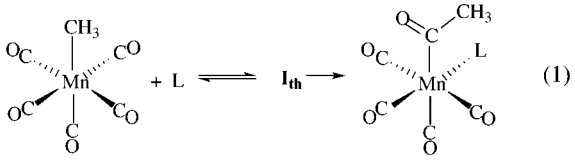

(1)

With an appropriate precursor, one can use photochemical techniques to prepare transient species with the same compositions as those proposed for specific reactive intermediates.[19] In this laboratory, we have used laser flash photolysis and time-resolved infrared (TRIR) or time-resolved optical (TRO) detection to interrogate the spectra and reaction dynamics of such reactive intermediates under conditions more directly relevant to the thermal reaction studies. As a caveat, the photochemical entry into these species is clearly different than a thermal path over the activation barrier, so one must critically evaluate where the entry method influences the structures and subsequent dynamic behavior of such reactive intermediates. Nonetheless, these techniques provide otherwise inaccessible opportunities to address directly the spectroscopic and dynamic properties of key intermediates, not only for model reactions such as that illustrated in eq 1, but also for true catalysts.[18]

Earlier TRO and TRIR investigations in this laboratory examined the spectra and ambient temperature dynamics of the transient ($\mathbf{I_{Mn}}$) generated upon CO photodissociation from the acyl precursor $CH_3C(O)Mn(CO)_5$ ($\mathbf{A_{Mn}}$) as illustrated in Scheme 1.[15] $\mathbf{I_{Mn}}$ has the same composition as intermediate(s) often proposed for eq 1,[3,4,11] and these studies demonstrated that, in weak donor solvents such as alkanes and halocarbons, it is stabilized by η^2-bonding of the acyl carbonyl. In the stronger donor tetrahydrofuran (THF), the spectroscopic and kinetics properties of $\mathbf{I_{Mn}}$ strongly suggest that it is the solvento intermediate, $CH_3C(O)Mn(CO)_4(THF)$. Here, we report further TRIR studies of this reaction using a high pressure, variable temperature (HPVT) sample cell[16] which allows much more exact control of the conditions and further TRO studies with a more stable detection system.

Scheme 1

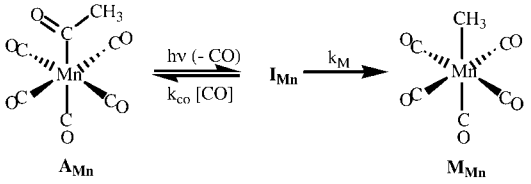

These improvements allowed measurement of the activation parameters for key steps in the decay of $\mathbf{I_{Mn}}$. In this context, the present study reports and compares activation parameters determined for the decay of $\mathbf{I_{Mn}}$ in two solvents, the weak donor cyclohexane (CH) and THF.

After our earlier study,[15] two theoretical (density functional) studies of migratory insertion intermediates discussed the possible importance of structures where agostic bonding of the acyl group alkyl function (e.g., the methyl group of $\mathbf{I_{Mn}}$) may stabilize intermediates in the migratory insertion.[13c,d] In an attempt to experimentally probe such intermediates, we have also carried out a more detailed comparison of the decay kinetics of the perprotio and perdeuterio forms of $\mathbf{I_{Mn}}$ generated by CO photodissociation.

Experimental Section

Materials. $CH_3C(O)Mn(CO)_5$ ($\mathbf{A_{Mn}}$) and $CD_3C(O)Mn(CO)_5$ ($\mathbf{A_{Mn}^d}$) were prepared following literature procedures.[22] All solvents were reagent grade and subjected to standard drying and distillation procedures.[23] Research grade carbon monoxide gas (99.995% purity from Spectra Gases) was used without further purification. Sample solutions for flash photolysis experiments were deoxygenated by entrainment with argon or carbon monoxide or by repeated freeze−pump−thaw cycles.

Time-Resolved Infrared Studies. The TRIR studies were conducted on an experimental apparatus that has been described previously.[18,20,21] The probe source consists of four lead-salt diode lasers that provide tunable infrared frequencies between 2200 and 1500 cm^{-1}. The IR beam is focused to a 7 mm diameter spot and overlapped at the plane of the sample cell with a slightly larger diameter 308 nm XeCl excimer pump pulse. The transmitted intensity of the probe beam is again focused to fill the 1 mm^2 active area of a photovoltaic Hg/Cd/Te detector. Changes in the transmitted IR intensity are recorded by a LeCroy LT342 digital storage oscilloscope.

A high pressure, variable temperature (HPVT) IR cell and flow system[17] was used in these studies. This system allows for the equilibration of sample solutions with gas pressures up to 100 atm and temperatures up to 150 °C. The large number of laser pulses required for signal averaging necessitated the flowing of the sample solutions at a rate of a few milliliters per minute through the HPVT cell in order to minimize complications due to accumulation and secondary photolysis of photoreaction products at the 3−4 Hz experimental cycle. The temperature of the solution was regulated in both the flow system and the HPVT TRIR cell.

(14) Webb, S. D.; Grandomencio, C. M.; Halpern, J. *J. Am. Chem. Soc.* **1986**, *108*, 34−5
(15) Boese, W. T.; Ford, P. C. *J. Am. Chem. Soc.* **1995**, *117*, 8381−91.
(16) McFarlane, K. L.; Lee, B.; Fu, W. F.; van Eldik, R.; Ford, P. C. *Organometallics* **1998**, *17*, 1826−34.
(17) Massick, S. M.; Ford, P. C. *Organometallics* **1999**, *18*, 4362−66.
(18) Massick, S. M.; Rabor, J. G.; Elbers, S.; Marhenke, J.; Bernhard, S.; Schoonover, J. R.; Ford, P. C. *Inorg. Chem.* **2000**, *39*, 3098−3106.
(19) (a) Hitam, R. B.; Narayanaswamy, R.; Rest, A. J. *J. Chem. Soc., Dalton Trans.* **1983**, 615−618. (b) McHugh, T. M.; Rest, A. J. *J. Chem. Soc., Dalton Trans.* **1980**, 2323−32.
(20) (a) DiBenedetto, J. A.; Ryba, D. W.; Ford, P. C. *Inorg. Chem.* **1989**, *28*, 3503−7. (b) Ford, P. C.; Bridgewater, J. S.; Lee, B. *Photochem. Photobiol.* **1997**, *65*, 57−64.
(21) Bridgewater, J. S.; Schoonover, J. R.; Netzel, T. L.; Massick, S. M.; Ford, P. C. *Inorg. Chem* **2001**, *40*, 1466−76.
(22) Gladysz, J. A.; Tam, W.; Williams, G. M.; Johnson, D. L.; Parker, D. W. *Inorg. Chem.* **1979**, *18*, 1163−65.
(23) Riddick, J. A.; Bunger, W. B.; Sakano, T. K. *Organic Solvents Physical Properties and Methods of Purification*, 4th ed.; John Wiley and Sons: New York, 1986; Vol. II.

Concentrations of the manganese solutions were typically 1−3 mM in cyclohexane for TRIR experiments, and initial absorbances were 0.3−0.4 for the most intense of the terminal carbonyl stretches of $\mathbf{A_{Mn}}$ for a 0.5 mm path length. Solutions were equilibrated in the flow system under various CO pressures (P_{CO}) for at least 45 min at temperatures ranging from 298 to 328 K. The CO concentrations in CH solutions were calculated from published solubility data.[24]

Time-Resolved Optical Experiments. The apparatus for the TRO experiments has been described previously.[21,25] A modification important to the present system involved using a 12 V battery powered 20 W halogen bulb with a dichroic reflector (GE FRE/CG) as the optical probe source. This source proved stable for the long acquisition times necessary for the slow processes that were problematic for the TRIR experiments. The excitation source was the third harmonic of a Nd:YAG laser (355 nm) crossed at 90° to the probe beam, which was chosen to be 1.5 times the diameter of the pump beam to minimize the effects of diffusion of species out of the detection region.

Solutions for the TRO experiments of 10−20 mL total volume were prepared in a custom fabricated 50 mL flask with an attached 1 cm quartz cell, were degassed by several freeze−pump−thaw cycles, and then were equilibrated with the appropriate gas on a vacuum manifold. The concentrations of $\mathbf{A_{Mn}}$ in CH and THF solutions were adjusted to 1−2 mM to provide absorbances of 0.2−0.4 at 412 nm. Typically, to minimize the number of laser pulses on the sample, 15 pulses per transient at approximately 1/min were averaged.

Results

TRIR Experiments. As shown previously,[15] pulsed laser photolysis of $\mathbf{A_{Mn}}$ in cyclohexane leads to CO photodissociation to give short-lived intermediate $\mathbf{I_{Mn}}$ with ν_{CO} bands at 1991(s), 1952(s), and 1607(w) cm^{-1}. $\mathbf{I_{Mn}}$ undergoes two primary decay paths: reaction with free CO to reform $\mathbf{A_{Mn}}$ (k_{CO}) and methyl migration from the acyl carbon to the metal to form $\mathbf{M_{Mn}}$ (k_M) in accord with Scheme 1. The temporal decays of $\mathbf{I_{Mn}}$ in CH under excess CO monitored at 1952 cm^{-1} were fit well by single exponentials. Extensive signal averaging was necessary to ensure accurate and precise k_{obs} values. In the present study, these were derived from averages of exponential fits for up to 26 separate decays, each being the average of 40−60 individual transients. The k_{obs} values and the standard deviations determined at various CO concentrations and temperatures appear in the plots shown in Figure 1.

According to Scheme 1, $k_{obs} = k_{CO}[CO] + k_M$, where k_{CO} is the bimolecular rate constant for reaction with CO and k_M is the unimolecular rate constant for methyl migration. Consistent with the model, plots of k_{obs} versus [CO] are linear at each temperature studied (Figure 1). Values for k_{CO} in cyclohexane were determined from linear least-squares fits of the k_{obs} versus [CO] plots for solutions equilibrated with CO gas pressures ranging from 11 to 31 atm (0.1 to 0.3 M). The high range of CO concentrations and the improved temperature regulation afforded by the HPVT IR cell and flow system resulted in more precise k_{CO} values than (although consistent with) previous measurements.[15,26] Values for k_{CO} determined from 298 to 328 K (Table 1) give a linear Eyring plot (Figure 2) from which activation parameters for k_{CO} were determined to be $\Delta H^{\ddagger}_{CO} = 31 \pm 1$ kJ mol^{-1} and $\Delta S^{\ddagger}_{CO} = -64 \pm 3$ J mol^{-1} K^{-1} in CH.

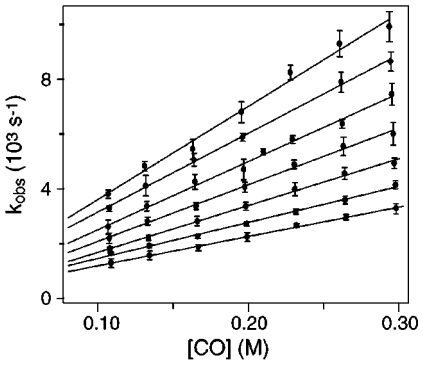

Figure 1. Overlay of the experimentally determined observed rate constant (k_{obs}) at various carbon monoxide concentrations and temperatures ranging from 25 to 55 °C.

Table 1. Rate Constants k_{CO} for CO Trapping of $\mathbf{I_{Mn}}$ To Give $\mathbf{A_{Mn}}$ in Cyclohexane and for Methyl Migration (k_M) of $\mathbf{I_{Mn}}$ To Give $\mathbf{M_{Mn}}$ in Cyclohexane and in THF

T (°C)	k_{CO} (cyclohexane)[a] (10^4 M^{-1} s^{-1})	k_M (cyclohexane)[b] (s^{-1})	k_M (THF)[b] (s^{-1})
25	1.07 (±0.02)	7.1 (±0.4)	24 (±1)
30	1.32 (±0.04)	9.0 (±0.4)	42 (±2)
35	1.62 (±0.09)	11.9 (±0.4)	71 (±7)
40	2.07 (±0.06)	14.4 (±0.6)	106 (±9)
45	2.49 (±0.09)	18.5 (±0.6)	142 (±10)
50	2.90 (±0.05)		
55	3.76 (±0.06)		
$\Delta H^{\ddagger}$ (kJ mol^{-1})	31 (± 1)	35 (± 1)	68 (± 4)
$\Delta S^{\ddagger}$ (J mol^{-1} K^{-1})	−64 (± 3)	−111 (± 3)	10 (± 10)

[a] Studies carried out using TRIR techniques with the HPVT cell. [b] Studies carried out using TRO techniques at low [CO] (see text).

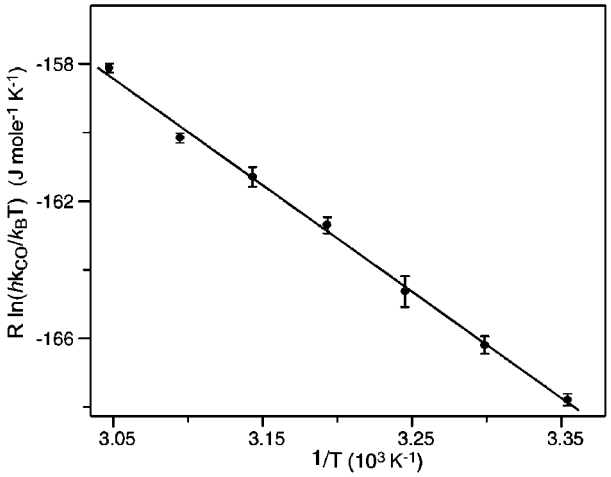

Figure 2. Eyring plot for the reaction of $\mathbf{I_{Mn}}$ with carbon monoxide (k_{CO}) in cyclohexane of the form R ln(hk_M/k_BT) vs T^{-1} (where R is the gas constant, h is the Plank constant, and k_B is the Boltzman constant).

(24) *IUPAC Solubility Data Series: Vol. 43. Carbon Monoxide*; Pergamon Press: Oxford, 1990.
(25) Lindsay, E.; Ford, P. C. *Inorg. Chim. Acta* **1996**, *242*, 51−56.
(26) In the earlier study by Boese,[15] the value $k_{CO} = 6.5 \pm 1.3 \times 10^3$ M^{-1} s^{-1} was reported for "room temperature" (~22 °C). This can be compared to the value $10.7 \pm 0.4 \times 10^3$ M^{-1} s^{-1} reported here for 25.0 °C cyclohexane. Given the different apparatus used as well as the greatly increased [CO] range of the present study, the agreement appears reasonable.

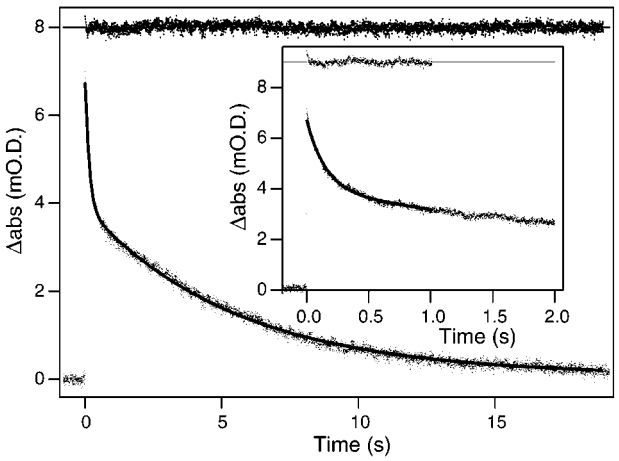

Figure 3. Absorbance changes at 410 nm following 355 nm photolysis of a cyclohexane solution of $\mathbf{A_{Mn}}$ equilibrated under argon at 298 K. The double exponential fits and residuals are included on both the long and short time scale acquisitions.

Analogous flash photolysis experiments on cyclohexane solutions of the deuterated analogue $CD_3C(O)Mn(CO)_5$ ($\mathbf{A_{Mn}}^{\mathbf{d}}$) were performed at 298 K. Single exponential decays were observed for the resulting intermediate ($\mathbf{I_{Mn}}^{\mathbf{d}}$), and the k_{obs} values measured gave a linear plot versus [CO]. Notably, the $k_{CO}{}^{d}$ value determined from the slope of that plot (1.09 ± 0.03) $\times$ 10^4 M^{-1} s^{-1} proved to be within experimental uncertainty of the value determined for $\mathbf{I_{Mn}}$ of (1.07 ± 0.02) $\times$ 10^4 M^{-1} s^{-1}; that is, the ratio $k_{CO}{}^{h}/k_{CO}{}^{d}$ (0.98 ± 0.04) in CH is indistinguishable from 1.00.

The linear fits of k_{obs} versus [CO] should have *y*-intercepts equal to the rate constant for methyl migration k_M, if $k_{CO}[CO] \ll k_M$ at low [CO]. While this proved to be the case, there was unsatisfactory scatter in the intercepts, which have relatively small values relative to the k_{obs} values measured experimentally. This resulted in part from limitations of the IR diode laser source stability which made acquisitions of transients with $\tau > 10$ ms problematic. Consequently, the data used to determine the k_{CO} values (Figure 1) were obtained on shorter time scales, that is, relatively high [CO] where $k_{CO}[CO] \gg k_M$. A similar observation was made by Boese.[15]

TRO Experiments. TRO detection proved more adaptable for measuring the slow rates at low [CO], especially once the battery powered probe source described in the Experimental Section was incorporated into the detection system. For this reason, the k_M values reported here were derived only from the TRO data. For these measurements, solutions of $\mathbf{A_{Mn}}$ were typically equilibrated under Ar, where $k_M = k_{obs}$ (see later), so the k_M values were measured by direct techniques and not by extrapolation of k_{obs} values measured at high [CO]. However, the relatively long data acquisition times ($\sim$1$-$10 s) led to complications due to diffusion from the detection region (k_{diff}). As a result, transient decays were modeled by double exponential functions as shown in Figure 3. The slower absorbance decay is due primarily to diffusion of product $\mathbf{M_{Mn}}$ out of the detection region at a rate much slower than the chemical processes corresponding to k_M (k_M/k_{diff} $\sim$33 at 298 K, $\sim$67 at 318 K). The diffusion process exhibited no [CO] dependence, a moderate temperature dependence, and, effectively, exponential decay rates. The differences in the magnitudes of k_M and k_{diff} were sufficiently large that it was necessary to use two time scales and an iterative procedure to obtain good quality double exponential fits. One time scale was chosen to be long enough to include at least several half-lives of the slowest decay (k_{diff}), while the shorter time scale was chosen to included 6$-$10 half-lives of the faster chemical process (k_{obs}). The longer time scale acquisition was fit to a double exponential function to obtain estimates of k_{obs} and k_{diff}. Then, the shorter time scale acquisition was fit to a double exponential while holding both the asymptote and k_{diff} constant to obtain a better estimate of k_{obs}. Next, improved values of the asymptote and k_{diff} were obtained by fitting the longer time scale acquisition to a double exponential holding only the improved value of k_{obs} constant, and so forth. Following this procedure, the k_{obs} values were found to rapidly converge after several iterations.

The efficacy of this fitting procedure to determine k_{obs} under such conditions can be evaluated from the k_{CO} calculated from these data. A plot of the k_{obs} values obtained by double exponential fits of TRO transients for $\mathbf{I_{Mn}}$ in cyclohexane (298 K) versus [CO] over the range 0 to 9.6 mM ($P_{CO} = 1$ atm) is linear, consistent with the expected relationship $k_{obs} = k_{CO}[CO] + k_M$. The value for k_{CO} determined in this manner ((1.02 ± 0.04) $\times$ 10^4 M^{-1} s^{-1}) compares very well to that ((1.07 ± 0.02) $\times$ 10^4 M^{-1} s^{-1}) determined by the TRIR technique. Because the much higher [CO] accessible in the HPVT-TRIR experiments resulted in fast single exponential decays for $\mathbf{I_{Mn}}$ unaffected by diffusion, the close agreement validates the correction procedure used in the TRO experiment to account for diffusion out of the detection region.

The k_M values for the decay of $\mathbf{I_{Mn}}$ in cyclohexane solution were obtained directly from the k_{obs} values measured for solutions equilibrated under an Ar atmosphere. In the absence of added CO, equating k_M and k_{obs} is justified only if the recombination of $\mathbf{I_{Mn}}$ with CO released photochemically has a negligible contribution to the decay of $\mathbf{I_{Mn}}$. This was tested by varying the photolysis laser pulse power to generate 5-fold differences in the initial $\mathbf{I_{Mn}}$ and CO concentrations. Inspection of the transient decay rates revealed no changes in the k_{obs} values resulting from contributions of a second-order process. Therefore, k_{obs} accurately represents k_M under these conditions. The methyl migration rate constants k_M thus measured in CH over the temperature range 298$-$318 K are listed in Table 1. The k_M value (298 K) determined in this manner is 7.1 ± 0.4 s^{-1}, and the activation parameters determined from linear least-squares fits of Eyring plots (Figure 4) are $\Delta H^{\ddagger}_M(CH) = 35 \pm 1$ kJ mol^{-1} and $\Delta S^{\ddagger}_M(CH) = -111 \pm 3$ J mol^{-1} K^{-1}.

The possible isotope effect on k_M was also evaluated by using the TRO technique to determine the reaction rates of intermediates generated from flash photolysis of the perdeuterated substrate $CD_3C(O)Mn(CO)_5$ ($\mathbf{A_{Mn}}^{\mathbf{d}}$) in cyclohexane. The $k_m{}^{d}$ value (298 K) measured was 7.3 ± 0.2 s^{-1}, which is within experimental uncertainty of the value found for the CH_3 analogue (7.1 ± 0.4 s^{-1}). Thus, the deuterium isotope

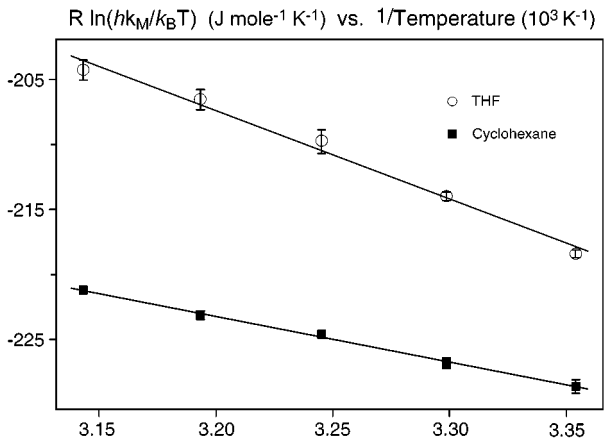

Figure 4. Eyring plots of the form $R \ln(hk_M/k_BT)$ versus T^{-1} for the methyl migration (k_M) of $\mathbf{I_{Mn}}$ in THF (○) and cyclohexane (■) equilibrated under Ar. (R is the gas constant, h is the Plank constant, and k_B is the Boltzman constant.) The temperatures range from 25 to 45 °C.

effect is deemed to be nearly negligible ($k_M{}^h/k_M{}^d$ (298 K) = 0.97 ± 0.05). Measurement of $k_M{}^d$ over the temperature range 298−318 K gave $\Delta H^{\ddagger}_M{}^d = 37 \pm 4$ kJ mol^{-1}and $\Delta S^{\ddagger}_M{}^d = -104 \pm 12$ J mol^{-1} K^{-1}, again within experimental uncertainties of the values determined for reactions of the perprotio compound. In other words, there were no differences in the methyl migration kinetics for the perprotio and perdeuterio $\mathbf{I_{Mn}}$ analogues in CH.

Analogous flash photolysis of $\mathbf{A_{Mn}}$ in tetrahydrofuran solution using TRO detection allowed for the measurement of k_M at various temperatures in this medium as well (Table 1). As reported by Boese,[15] the value of k_{CO} in THF (~4 × 10^2 M^{-1} s^{-1}) is considerably smaller than in cyclohexane and could not be accurately measured at the low CO obtained from $P_{CO} \leq 1$ atm, while other technical problems prevented its measurement at higher P_{CO} on the TRIR apparatus using the HPVT cell.[27] However, by using the TRO apparatus, it was possible to measure the rates of methyl migration for $\mathbf{I_{Mn}}$ in THF at various T. Notably, methyl migration was found to be both faster at 298 K ($k_M = 24 \pm 1$ s^{-1}) and more temperature dependent in THF than in CH (7.1 ± 0.4 s^{-1}). The Eyring plot for k_M (Figure 4) gave the activation parameters $\Delta H^{\ddagger}_M$(THF) = 68 ± 4 kJ mol^{-1} and $\Delta S^{\ddagger}_M$(THF) = 10 ± 10 J mol^{-1} K^{-1}.

Discussion

As noted in the Introduction, much discussion regarding intermediates in the migratory insertion mechanism has been concerned with three limiting structural types having the "vacant" coordination site occupied by the oxygen of an η^2-acyl carbonyl, by a solvent molecule or by agostic interaction with a carbon−hydrogen bond of the acyl methyl group. For the manganese intermediate $\mathbf{I_{Mn}}$, these are illustrated as **C**, **S**, and **B**, respectively.

Earlier studies from this laboratory[15] demonstrated that the TRIR spectra and the kinetics behavior of the transient species $\mathbf{I_{Mn}}$ generated by photodissociation of CO from $\mathbf{A_{Mn}}$ are dependent on the solvent. In cyclohexane and other

(27) THF degrades the seals used in the HPVT cell and flow system.

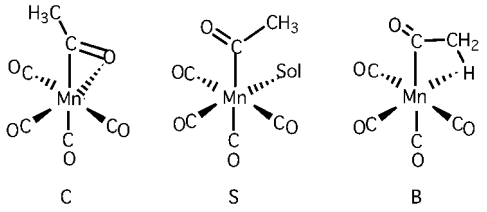

weakly coordinating solvents, the structure was concluded to be η^2-acyl complex **C**. This conclusion was based on the TRIR spectra recorded for $\mathbf{I_{Mn}}$ and on the reaction dynamics of this species. For example, there is a −59 cm^{-1} shift of the acyl group ν_{CO} band on going from $\mathbf{A_{Mn}}$ to $\mathbf{I_{Mn}}$, in CH, consistent with differences seen for systems where mono- and dihapto-acyl coordination can be compared for similar metal centers.[28,29] In addition, the kinetics of trapping by CO and by other ligands L are sluggish relative to the rates expected for a solvento complex in cyclohexane. The low reactivity of $\mathbf{I_{Mn}}$ is pronounced by comparison to the intermediate **X** formed by flash photolysis of $\mathbf{M_{Mn}}$ (eq 2) and was concluded to be solvento complex *cis*-$CH_3Mn(CO)_4$(Sol).[15,30] **X** is 5 orders of magnitude more reactive toward CO ($k_{CO} = 4.5 \times 10^8$ M^{-1} s^{-1}) than is $\mathbf{I_{Mn}}$ (1.07 × 10^4 M^{-1} s^{-1}) in 298 K CH. Furthermore, while k_{CO} values for **X** are markedly solvent dependent, those for $\mathbf{I_{Mn}}$ are nearly solvent independent in relatively weak donor solvents such as hydrocarbons and halocarbons. The exception is THF in which the reactivity of $\mathbf{I_{Mn}}$ with CO is (at least) a factor of 20 smaller than in CH while the reactivity with $P(OMe)_3$ is 3 orders of magnitude lower.[15]

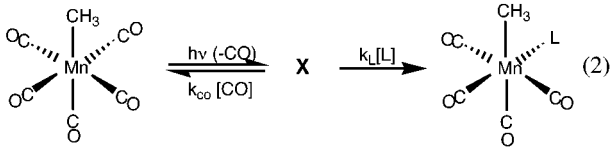

While η^2-acyl chelation (**C**) would explain the relative stability toward reaction with incoming ligands in weakly coordinating solvents as well as the TRIR spectrum of $\mathbf{I_{Mn}}$, the agostic chelate **B** cannot be excluded off-hand. Computations using density functional methods[13d] concluded that **C** is significantly lower in energy than **B** and agreed that **C** was the likely structure of $\mathbf{I_{Mn}}$ formed by the photodecarbonylation mechanism. These calculations furthermore indicated that, if **B** were formed, it would be very short-lived (see later). Notably, in related time-resolved spectroscopy studies of cobalt catalyst models,[18] photolysis of $CH_3C(O)Co(CO)_3PPh_3$ in various solvents leads to the "unsaturated" intermediate $CH_3C(O)Co(CO)_2PPh_3$ ($\mathbf{I_{Co}}$), which is also apparently stabilized by the η^2-acyl coordination.

Reactions in Cyclohexane. Comparison of the activation parameters for k_M and k_{CO} for $\mathbf{I_{Mn}}$ measured in CH presents an interesting contrast. The activation enthalpies are similar: 35 kJ mol^{-1} for k_M, 31 kJ mol^{-1} for k_{CO}. However, the

(28) Hermes, A. R.; Girolami, G. S. *Organometallics* **1987**, *7*, 394.
(29) Boese, W. T.; Ford, P. C. *Organometallics* **1994**, *13*, 3525−31.
(30) Replacement of a π-acid ligand such as CO by a stronger σ-donor, weak π-donor ligand such as THF would shift both terminal and on acyl ν_{CO} frequencies to lower values.

Scheme 2

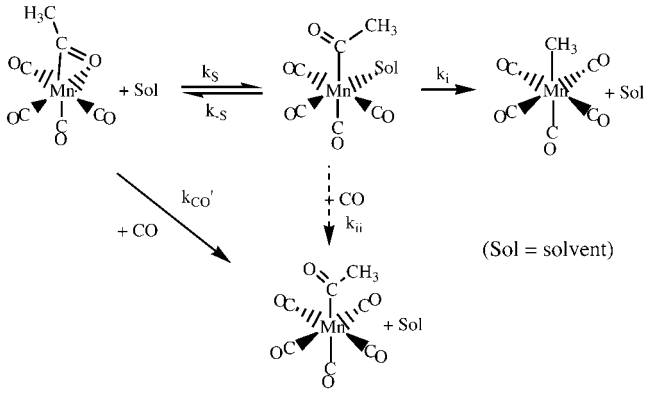

$\Delta S^{\ddagger}$ values are substantially different, with the "unimolecular" methyl migration step having the considerably more negative entropy of activation. This would be consistent with the argument that methyl migration from $\mathbf{I_{Mn}}$ in weakly coordinating solvents is not unimolecular but involves coordination of a solvent molecule to facilitate the rearrangement of the acyl group to a conformation better suited for methyl migration to the metal (see later). The similarity in activation enthalpies suggest competitive processes where the dominant enthalpy contribution to each is due to dissociation of the Mn···O bond of the η^2-acyl complex.

A possible model for these transformations in cyclohexane is illustrated in Scheme 2.

For this model where $\mathbf{I_{Mn}} = \mathbf{C}$, the rate law for $\mathbf{I_{Mn}}$ decay is derived from steady-state kinetics applied to [**S**]:

$$-\left(\frac{d[\mathbf{C}]}{dt}\right) = \left(\frac{k_i k_S}{k_i + k_{-S} + k_{ii}[CO]} + \frac{k_{ii} k_S [CO]}{k_i + k_{-S} + k_{ii}[CO]} + k'_{CO}[CO]\right)[\mathbf{C}] = k_{obs}[\mathbf{C}] \quad (3)$$

However, because there was no curvature to the plots shown in Figure 1, k_{ii}[CO] must be much smaller than $k_i + k_{-S}$ for all [CO] investigated. Furthermore, the earlier studies clearly demonstrated that for a series of hydrocarbon and halocarbon solvents in which $\mathbf{I_{Mn}}$ was concluded to be **C**, k_M was dependent on the nature of the solvent while k_{CO} was little affected. Thus, we conclude that the k_{ii} pathway must be at most a minor pathway to $\mathbf{A_{Mn}}$, so k_{obs} can be rewritten as

$$k_{obs} = \frac{k_i k_S}{k_i + k_{-S}} + k'_{CO}[CO] = k_M + k_{CO}[CO] \quad (4)$$

In this context, the reformation of $\mathbf{A_{Mn}}$ that occurs via the k_{CO} pathway would appear to be a simple direct displacement of the η^2-acyl oxygen by CO in an associative mechanism. This would be consistent with the negative value of $\Delta S^{\ddagger}_{CO}$. It is notable that the $\Delta H^{\ddagger}_{CO}$ value determined here (31 kJ mol^{-1}) for $\mathbf{I_{Mn}}$ compares favorably to the barrier of 26 kJ mol^{-1} calculated[13d] for the reaction of **C** with CO to reform $\mathbf{A_{Mn}}$ via an analogous direct displacement mechanism.

A large negative entropy of activation would also be expected for the k_M pathway if the rate-limiting step were simple solvent displacement of the η^2-acyl oxygen by CH, that is, the k_S step. However, it is not clear that in such a case the value of $\Delta S^{\ddagger}_S$ would be expected to be substantially more negative than $\Delta S^{\ddagger}_{CO}$. An alternative way to treat this pathway would be to assume that the first step is a preequilibrium (i.e., that $k_i \ll k_{-S}$) and that $k_M = k_i k_S/k_{-S}$. If this were the case, then $\Delta H^{\ddagger}_M = \Delta H^{\ddagger}_S + \Delta H^{\ddagger}_I - \Delta H^{\ddagger}_{-S}$ and $\Delta S^{\ddagger}_M = \Delta S^{\ddagger}_S + \Delta S^{\ddagger}_I - \Delta S^{\ddagger}_{-S}$. (The third terms are less straightforwardly defined if $k_i \sim k_{-S}$). The activation parameters for such multistep reactions include contributions from each step, and the more negative value of $\Delta S^{\ddagger}_M$ may be reflective of a highly ordered transition state for the k_i step.

The role of agostic stabilization of the transition state for the k_M step may in principle be probed by the isotope labeling experiment. According to the previous kinetics treatment, $k_M = k_i k_S/k_{-S}$ for the conversion of **C** to $\mathbf{M_{Mn}}$, but only the k_i term should be sensitive to isotopic labeling. The absence of an isotope effect might argue against a significant role of agostic bonding in determining the activation barriers of these reactions, but it is not clear that the precision of the measurements is sufficient to make a strong case in this regard (see later).

Reactions in Tetrahydrofuran. As noted previously, the TRIR spectrum as well as the much lower reactivity toward CO led to the conclusion that $\mathbf{I_{Mn}}$ is the solvento species **S** in THF.[15] Interestingly, a recent density functional study[13d] using the Gaussian 94 program concluded that η^2-acyl chelate **C** should be the more stable species even in THF and argued that our earlier assignment as a solvento species was incorrect. However, if this were the case, the reaction rate of $\mathbf{I_{Mn}}$ with CO to reform $\mathbf{A_{Mn}}$ should not be significantly different in THF than in the other solvents. *This argument is clearly in contradiction to the experimental observations*. As noted previously, the reaction of $\mathbf{I_{Mn}}$ with CO is at least a factor of 20 slower in THF than the comparable reaction in CH, while the second-order k_L for the trapping of $\mathbf{I_{Mn}}$ by $P(OMe)_3$ is 3 orders of magnitude lower in THF than in cyclohexane at ambient temperature.[15] *Thus, the theoretical treatment as offered by ref 13d falls significantly short of describing the experimental observations in this case.*

On the other hand, we need to address the seemingly ambiguous result that the ambient temperature k_M values for the methyl migration pathway are rather similar in CH and THF solutions (7.1 s^{-1} and 24 s^{-1}, respectively, at 298 K). This apparent similarity is completely dispelled by comparing the activation parameters, which are $\Delta H^{\ddagger}_M$(CH) = 35 ± 1 kJ mol^{-1} and $\Delta S^{\ddagger}_M$(CH) = −111 ± 3 J mol^{-1} K^{-1} versus $\Delta H^{\ddagger}_M$(THF) = 68 ± 4 kJ mol^{-1} and $\Delta S^{\ddagger}_M$(THF) = 10 ± 10 J mol^{-1} K^{-1}. Thus, the slower methyl migration rate in cyclohexane at 298 K can be attributed to the much less favorable entropy of activation. Because limitations on the temperature range and precision of k_M measurements add uncertainty in the data extrapolation necessary to obtain activation entropies, one must be wary of overinterpreting $\Delta S^{\ddagger}$ values. However, the substantial differences in both $\Delta S^{\ddagger}$ and $\Delta H^{\ddagger}$ lead us to conclude with confidence that there is a change in mechanism for the methyl migration reaction of $\mathbf{I_{Mn}}$ upon going from CH to THF. *That change can be*

Scheme 3

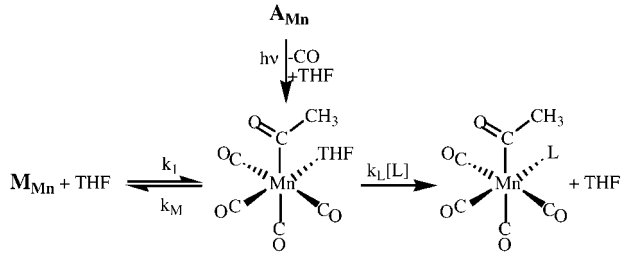

*attributed to different I_{Mn} structures, **C** and **S**, generated upon photolysis of A_{Mn} in CH and THF, respectively.*

Relevance to the Thermal Migratory Insertion Mechanism. What is the relationship between the photochemically generated transient described here ($\mathbf{I_{Mn}}$) to the intermediate(s) ($\mathbf{I_{th}}$) formed along the reaction coordinate of thermal carbonylation (eq 1)? A test of this would be to make a quantitative reactivity comparison of $\mathbf{I_{Mn}}$ and $\mathbf{I_{th}}$ under analogous conditions. Specifically, if these transients show the same selectivity between methyl migration (k_M) and ligand addition (k_L), then the two intermediates are likely to be the same. This was demonstrated[15] by comparing the branching ratio k_M/k_L from the steady-state kinetics of the thermal reaction of $\mathbf{M_{Mn}}$ with $P(OMe)_3$ in solvent THF (eq 1) to that for the photochemically generated species $\mathbf{I_{Mn}}$ for which the values of k_M and k_L could be determined directly. The branching ratios were the same; therefore, the intermediate observed for the photochemical experiment in THF can be concluded to be the same as that formed in the thermal reaction in this media, namely the solvento complex **S** (Scheme 3).

The situation is entirely different in a weakly coordinating solvent such as cyclohexane where $\mathbf{I_{Mn}}$ was concluded to be the η^2-acyl chelate complex **C**. As discussed before,[15] **C** does not appear to lie on a direct pathway between $\mathbf{M_{Mn}}$ and $\mathbf{A_{Mn}}$, despite the general concurrence that it is the lowest energy species having the composition $CH_3C(O)Mn(CO)_4$ in weakly donating solvents. The reaction of **C** (generated photochemically) to form $\mathbf{M_{Mn}}$ shows kinetic sensitivity to the relative donor properties of these media in a manner that suggests direct solvent interaction with the metal center in the k_M step as illustrated by Scheme 2. Although this is consistent with earlier reports of solvent effects on thermal migratory insertion, it is entirely possible that the thermal reaction, which is quite slow in such media, is a concerted pathway involving associative attack of the incoming ligand with no kinetically viable intermediates.

In previous experimental kinetics studies in hydrocarbon solutions,[4,15] the reaction of **M** with different L proved to be strictly second-order over the ligand concentrations studied. While this behavior would be consistent with nucleophilic attack of L concerted with methyl migration, a kinetically consistent alternative would be unimolecular formation of $\mathbf{I_{th}}$, followed by reaction with L, if the constraint $k_M \gg k_L[L]$ were met. The rate constants for $\mathbf{I_{Mn}}$ in cyclohexane derived in the photochemical experiment do not meet this constraint either for L = CO (this work) or for L = $P(OMe)_3$.[15] Thus, this suggests that, unlike the reactions in THF, intermediate **C** seen in the TRIR and TRO experiments in CH is not an intermediate for the thermal pathway under these conditions. Instead, a concerted mechanism, such as associative attack of L on the Mn, appears more plausible, although a less direct pathway such as nucleophilic activation of a carbonyl is difficult to exclude.[14,31]

The reported Gaussian-94 based density functional computations[13d] appear to support such a pathway in the absence of a donating solvent. This report concluded that the reactive intermediate in the thermal reaction is **B** and that, although **C** was found to be lower energy, the barrier to form **C** from $\mathbf{M_{Mn}}$ is large. However, the calculations placed **B** in a potential energy minimum so shallow (0.1 kcal mol^{-1}) that it is incorrect to view this as a reactive intermediate, because $kT = 0.6$ kcal mol^{-1} at ambient temperature. Although interpreted differently by the authors, the reaction coordinate profile described by the computation[13d] is essentially that of concerted addition of CO to $\mathbf{M_{Mn}}$ with the transition state stabilized somewhat by agostic interaction between the methyl and Mn.

In summary, the reaction dynamics of the transient species $\mathbf{I_{Mn}}$ generated by flash photolysis of $CH_3C(O)Mn(CO)_5$ show different activation parameters in cyclohexane and THF owing to their different structures in these media, the chelate species **C** in the former, the solvento species **S** in the latter. In CH, $\Delta H^{\ddagger}$ values are similar for k_M (35 kJ mol^{-1}) and k_{CO} (31 kJ mol^{-1}), but $\Delta S^{\ddagger}$ values are substantially different, with "unimolecular" methyl migration having the considerably more negative entropy of activation. This would be consistent with a mechanism by which methyl migration from **C** in weakly coordinating solvents requires solvent coordination to facilitate the rearrangement of the acyl group to a conformation better suited for methyl migration. In THF, the k_M pathway gave considerably different activation parameters from those in CH with $\Delta H^{\ddagger}_M = 68 \pm 4$ kJ mol^{-1}. This is consistent with the earlier conclusion[15] that the composition of $\mathbf{I_{Mn}}$ is different in these two media. The possible isotope effect on k_M was also evaluated by studying the intermediates generated from flash photolysis of $CD_3C(O)Mn(CO)_5$ in CH, but this was found to be nearly negligible. The absence of an isotope effect argues against a significant role of agostic bonding in determining the activation barriers of these reactions within the relatively high precision of the current measurements.

Acknowledgment. This research was sponsored by a grant (DE-FG03-85ER13317) from the Division of Chemical Sciences, Office of Basic Energy Sciences, U.S. Department of Energy.

IC020116R

(31) Ford, P. C.; Rokicki, A. *Adv. Organomet. Chem.* **1988**, *28*, 139−217